Journal of Robotics and Control (JRC)
Volume 6, Issue 3, 2025
ISSN: 2715-5072, DOI: 10.18196/jrc.v6i3.26493

Robust Velocity Control of Rehabilitation Robots Using Adaptive Sliding Mode and Admittance Strategies

I. V. Merkuryev [1], T. B. Duishenaliev [2], Guijun Wu [3*], Zh. Zh. Dotalieva [4], A. A. Orozbaev [5]
[1, 2] Department of Robotics, Mechatronics, Dynamics and Strength of Machines, National Research University Moscow Power Engineering Institute, Moscow,111250, Russia
[3, 4, 5] Department of Mechanics and Industrial Engineering, Kyrgyz-German Technical Institute, Kyrgyz State Technical University named after I. Razzakov, Bishkek, 720044, Kyrgyzstan
[3] Department of Mechanical Engineering, Anyang Institute of Technology, Anyang, Henan, 455000, China
Email : [1] merkuryeviv@mpei.ru, [2] duyshenaliyevt@mpei.ru, [3] wuguijun957@gmail.com, [4] zh.dotalieva@kstu.kg
*Corresponding Author

Abstract*—This paper investigates a velocity tracking control strategy for a planar rehabilitation training robot equipped with two independent linear actuators along the X and Y axes. A dual-loop control framework is proposed by combining admittance control and adaptive sliding mode robust control to facilitate compliant and accurate human–robot interaction during active rehabilitation. In the outer loop, admittance control converts the interaction force applied by the patient into a reference velocity, enabling compliant force-to-motion mapping. In the inner loop, an adaptive sliding mode controller augmented with a disturbance observer is designed to ensure robust tracking performance under model uncertainties and external disturbances. Lyapunov theory is employed to prove the closed-loop stability, ensuring that tracking errors asymptotically converge to zero. Compared to conventional PID control, the proposed method reduces the root mean square tracking error (RMSE) from 0.2113 m/s to 0.0747 m/s(a 64.6% reduction), decreases the maximum velocity error from 0.4553 m/s to 0.2057 m/s(a 54.8% reduction), and shortens the recovery time after disturbances from 1.26 s to 0.81 s, as validated through MATLAB simulations. Preliminary experimental results on a planar upper-limb rehabilitation robot demonstrate the controller's real-time applicability and confirm its effectiveness in improving interaction responsiveness and motion stability. Nevertheless, the implementation introduces increased computational complexity and may require real-time optimization for deployment on embedded systems. Furthermore, while this study focuses on planar motion, the control framework can be extended to multi-DOF systems and integrated with physiological signal-based intention recognition to enable more personalized rehabilitation. These results indicate that the proposed strategy offers a promising solution for enhancing the performance, robustness, and adaptability of rehabilitation robots in clinical and home-care applications, though clinical trials have not yet been conducted.

Keywords—Rehabilitation Robot; Admittance Control; Adaptive Sliding Mode Control; Disturbance Observer; Velocity Tracking; Human–Robot Interaction; Lyapunov Stability; Multi-DOF Systems.

I. INTRODUCTION

Neurological disorders such as stroke and spinal cord injury have resulted in a growing global population suffering from motor impairments and reduced mobility [1]–[3]. Clinical studies have demonstrated that high-intensity, repetitive, and task-specific rehabilitation training can effectively promote neuroplasticity and enhance motor recovery [4], [5]. To overcome the limitations of traditional manual therapy—such as low training intensity, inconsistent therapist input, and limited scalability—rehabilitation robots have emerged as intelligent solutions that integrate mechanical systems [6]–[8], control theory, and artificial intelligence [9], [10]. These systems provide consistent, high-frequency interventions, offering great promise in improving patient outcomes [11]–[14].

Despite their advantages, most existing rehabilitation robots face two critical challenges. First, it is difficult to achieve compliant and adaptive human–robot interaction (HRI) in the presence of variable patient input [15], [16], fatigue, or intent. Second, these systems often exhibit low robustness to model uncertainties and external disturbances, which can compromise tracking accuracy and safety [17]–[22]. Therefore, among compliance-oriented strategies, admittance control has gained widespread application due to its ability to convert human-applied interaction forces into motion commands. Several studies have enhanced admittance control by incorporating adaptive and personalized mechanisms. For example, Wu et al. introduced a minimal-intervention strategy to support patient autonomy [10]; Han et al. proposed a muscle-strength-based adaptive scheme to respond to fatigue [23]; Zhang et al. integrated EMG-based motion intention recognition to personalize training [24]; and Lee et al. employed convolutional neural networks to optimize admittance parameters from patient motion data [25]. However, these methods remain vulnerable to external disturbances and unmodeled dynamics, and often lack mechanisms to ensure robust tracking under real-world uncertainties. In contrast, sliding mode control (SMC) is well known for its robustness against system uncertainties and perturbations [26]–[30]. By constraining system trajectories onto a sliding surface, SMC guarantees convergence even in the presence of bounded disturbances. Research in recent years has improved SMC performance through dynamic sliding surfaces [31], adaptive gain tuning [32], and the

integration of disturbance observers, such as extended state observers (ESO) and nonlinear disturbance observers (NDO) [33], [34]. These techniques enhance robustness and reduce chattering effects. Nonetheless, classical SMC still suffers from residual chattering and assumes ideal disturbance estimation, which may not hold under dynamic, nonlinear human–robot interactions [35]–[37].

Traditional PID controllers, despite their simplicity and popularity, struggle with model mismatches and fail to maintain stable tracking performance during episodes of spasticity or parameter variation [38].

While previous efforts have attempted to combine admittance control and SMC, a systematic framework that unifies compliant interaction with adaptive robustness and disturbance rejection remains underdeveloped [39]–[41]. Many existing hybrid approaches lack adaptive tuning, depend on heuristic parameter settings, or omit the explicit role of disturbance estimation [42]–[44]. Moreover, few existing studies evaluate the trade-offs between compliance, tracking accuracy, and computational overhead, which are critical considerations for real-time implementation in embedded systems used in rehabilitation scenarios [45], [46]. Addressing this balance is essential to ensure both control effectiveness and practical feasibility.

To address these limitations, this paper proposes a robust velocity tracking control strategy for a two-degree-of-freedom planar rehabilitation robot based on a dual-loop architecture:

- An outer-loop admittance controller transforms interaction force into a reference velocity to achieve compliant HRI [47], [48];
- An inner-loop adaptive sliding mode controller, augmented by a disturbance observer, ensures robust and accurate tracking performance under model uncertainties and external disturbances;
- A Lyapunov-based stability analysis is provided to verify the asymptotic convergence of velocity tracking errors.

Compared with conventional PID and fixed-gain SMC controllers, the proposed method demonstrates superior tracking accuracy, improved robustness, and better adaptability under varying interaction forces, as validated by simulation and preliminary experimental results. This control framework offers a practical solution for enhancing the responsiveness and reliability of rehabilitation robots in active, patient-centered training.

The major contributions of this paper are summarized as follows:

- A dual-loop control strategy combining admittance control and adaptive SMC is proposed for planar rehabilitation robots.
- A disturbance observer is integrated to enhance robustness and reduce chattering under uncertain dynamics.
- Lyapunov-based stability analysis is provided for the proposed controller.
- Simulation and experimental results validate the system's compliance and adaptability under spastic or varying patient force input.

This hybrid strategy improves safety and tracking precision, enabling safer, higher-intensity training for patients with motor impairments or muscle spasms.

The rest of the paper is structured as follows. Section II presents the system modeling and the dual-loop control design; Section III reports simulation and experimental validation results; Section IV discusses performance, limitations, and future work; Section V concludes the paper.

II. METHOD

A. System Modeling and Controller Design

Before designing the controller, we need a mathematical model that describes how the robot moves in response to applied forces. This model serves as the foundation for developing precise and responsive control strategies [49], [50]. In this section, the dynamic model of the planar rehabilitation robot is first established. Then, the admittance-based outer-loop control mechanism, which converts human–robot interaction force into reference velocity, is explained. Finally, the design of the adaptive sliding mode robust controller is presented, including the definition of the sliding surface, derivation of the control law, and construction of the disturbance observer.

B. Dynamic Modeling

To capture the robot's motion, we analyze how forces along the X and Y axes cause acceleration, based on Newton's second law. The system is simplified using decoupling assumptions to reduce computational complexity [51], [52]. The rehabilitation robot in this study is designed as a 2-DOF planar system, consisting of two orthogonally arranged and independently actuated translational modules. To analyze the dynamic interactions between the two axes, a general coupled dynamic model is formulated as:

$$\begin{bmatrix} m_x & m_{xy} \\ m_{yx} & m_y \end{bmatrix} \begin{bmatrix} \ddot{x} \\ \ddot{y} \end{bmatrix} + \begin{bmatrix} d_x & d_{xy} \\ d_{yx} & d_y \end{bmatrix} \begin{bmatrix} \dot{x} \\ \dot{y} \end{bmatrix} = \begin{bmatrix} F_x \\ F_y \end{bmatrix} \quad (1)$$

The terms m_{xy},m_{yx}, d_{xy},and d_{yx} represent the cross-axis inertial and damping coupling terms. This matrix-based formulation is widely used in multivariable mechanical systems, including robotic manipulators and mechatronic platforms [53], [54].

Preliminary experimental tests and structural symmetry analysis indicate that these coupling terms are relatively small, Thus, the coupled model can be approximated as dynamically decoupled:

$$m_x \cdot \ddot{x} = F_x \qquad m_y \cdot \ddot{y} = F_y \quad (2)$$

This simplification allows for independent controller design on each axis and significantly reduces computational complexity during real-time implementation.

The structure of the two-dimensional upper limb rehabilitation robot discussed in this study is shown in Fig. 1.

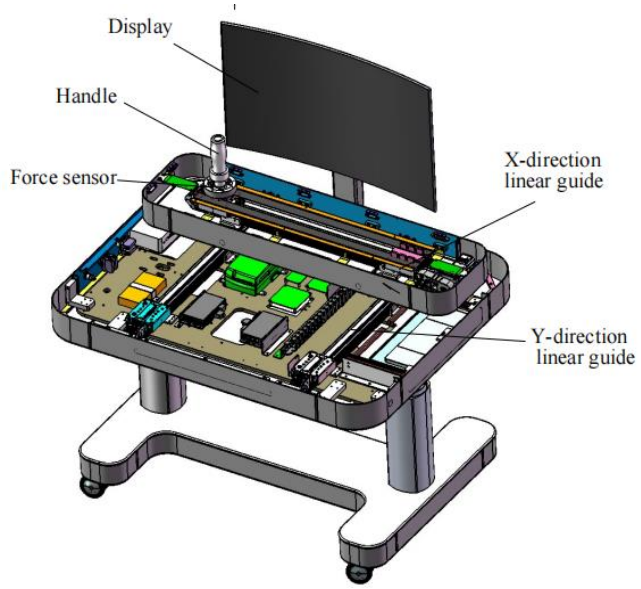

Fig. 1. Two-dimensional upper limb rehabilitation robot discussed

The upper-limb rehabilitation robot supports four training modes: active movement, passive movement, resistive mode, and assistive mode. Among these, the active movement mode is the most frequently used. In this mode, the patient is required to actively move the handle within the planar workspace to perform tasks such as drawing circles or moving along straight lines, which demands the highest level of velocity tracking accuracy from the control system.

The two linear drive axes are treated as dynamically decoupled based on the platform's orthogonal linear guide structure and minimal mechanical coupling [55], [56].

$$m_x \ddot{q}_x = F_m + F_{ex} - d_x \tag{3}$$

where $\ddot{q}_x$ denotes the acceleration of the handle along the X-axis, and m_x represents the equivalent inertial mass of the handle in the X direction, i.e., the mass of the handle. F_m is the driving force applied by the linear actuator along the X-axis; F_{ex} is the interaction force exerted by the patient along the X-axis; and d_x represents the total disturbance and uncertainties along the X-axis, which may include unmodeled friction, parameter variations, and external environmental disturbances, etc. Similarly, the dynamic model in the Y-axis direction is:

$$m_y \ddot{q}_y = F_m + F_{ey} - d_y \tag{4}$$

The physical meanings of each variable are similar to those in the X-axis, differing only in the direction of action. Since the two axes are independently controlled, the subsequent controller design process is identical for both the X and Y axes. The following sections will focus on the derivation of the control method for the X-axis.

C. Admittance Control Outer-Loop Design

The outer-loop admittance controller translates the human-applied interaction force into a target velocity for the robot. This mimics how a physical system with mass and damping responds to force, making interaction more natural and compliant. Admittance control introduces an equivalent mechanical impedance model into the robot control system to compute the robot's motion response based on the force applied by the human [57]–[60]. In this study, a second-order linear admittance model is adopted to convert the interaction force into the desired velocity command. For each axis, virtual inertia M_d and damping coefficient B_d are defined to represent the expected dynamic compliance relationship. When a force F_{ex} is applied in a given direction, the expected velocity response of the robot satisfies the following admittance model equation:

$$M_d \dot{v}_d + B_d v_d = F_{ex} \tag{5}$$

Here, v_d is the desired velocity of the robot along the X-axis as calculated by the admittance controller, and $\dot{v}_d$ is its rate of change (i.e., acceleration). Equation (5) describes a first-order inertia–damping system: when a patient applies a constant interaction force to the handle, the handle of the rehabilitation robot will move at a steady velocity, the magnitude of which is determined by B_d. At steady state, $\dot{v}_d = 0$:

$$B_d v_d = F_{ex}$$

When the applied force increases suddenly, the virtual inertia M_d limits the instantaneous rate of velocity change, making the acceleration process smoother and preventing unsafe rapid motion. By adjusting the values of M_d and B_d, different equivalent mechanical admittance characteristics can be set:

A larger B_d provides greater damping (i.e., lower compliance, requiring the patient to apply more force to move the robot quickly); A smaller B_d results in higher compliance (i.e., allowing the robot to respond to smaller forces more easily); The inertia M_d affects the inertial response of the system — if too large, the system may respond too sluggishly; if too small, the system may become overly sensitive to small force variations.

In this study, appropriate admittance parameters are selected based on the needs of rehabilitation training [61], [62], ensuring that the robot's response to the patient's force output is neither too stiff nor too sensitive, thus maintaining smooth and safe human–robot interaction.

In implementation, the admittance controller serves as the outer loop, taking the real-time measured human–robot interaction force F_{ex} as input and solving the differential equation (5) online to obtain the desired velocity v_d. In discrete-time systems, numerical integration methods can be used to iteratively calculate v_d; for example, using the Euler method [63]–[65], the following is executed at each control period Δt:

$$v_{(t+\Delta t)} = v_{(t)} + \frac{\Delta t}{M_d}(F_{ex} - B_d v_{(t)}) \tag{6}$$

To compute how the robot should move in response to force in real time, we use numerical integration to update the desired velocity at each control step [66]–[68]. Although the Euler method is used for real-time numerical integration due to its simplicity, its accuracy is controlled by adopting a sufficiently small sampling interval (e.g., 1 ms). Given the relatively slow dynamics of upper-limb motion, this high-frequency regime ensures numerical stability and acceptable

accuracy for real-time admittance control, as validated in simulation and hardware-in-the-loop tests.

Through this outer-loop admittance control, the robot is able to "yield" to the force applied by the patient, moving with the specified inertia and damping characteristics, thereby achieving a compliant force-to-velocity transformation [69], [70].

D. Inner-Loop Design of Adaptive SMC

The outer-loop admittance control generates the desired velocity signal v_d, but the robot's actual motion velocity $v_i = \dot{q}_i$ still needs to be tracked by the inner-loop controller. Considering the presence of model uncertainties and external disturbances, this study adopts SMC as the inner-loop velocity tracking strategy, and introduces adaptive tuning and a disturbance observer to enhance robustness and reduce chattering [71]–[73]. The design process of the sliding mode controller is detailed below.

1) Sliding Surface and Error Definition:

Let the difference between the actual velocity v_i of the X-axis and the desired velocity v_d be defined as the tracking error:

$$e_i = v_d - v_i \tag{7}$$

Since the control objective is to ensure that the actual velocity closely follows the desired velocity, it is expected that $e_i \to 0$. To ensure accurate tracking and fast response, we define a sliding surface that combines the current tracking error, its rate of change, and the accumulated error over time [74]. This allows the controller to react to both sudden changes and long-term trends in the error, enhancing stability and eliminating steady-state error. To improve the dynamic response and robustness against disturbances, a first-order proportional–integral (PI) sliding surface is introduced, defined as:

$$s = e_i + \lambda \dot{e}_i + \rho \int_0^t e_i(t)dt \tag{8}$$

where $\lambda > 0$ is the proportional gain, and $\rho > 0$ is the integral gain, used to enhance system stability and the ability to eliminate steady-state errors.

This sliding surface not only includes the velocity tracking error e_i, but also incorporates its rate of change $\dot{e}_i$ and an integral term, enabling it to better reflect the dynamic variation of the tracking error in the system. The control objective is to ensure $s \to 0$, thereby achieving $e_i \to 0$.

2) Control Law Design:

The total control force is designed to track the reference velocity generated by the admittance controller, while compensating for external disturbances and ensuring stability [75], [76]. When constructing the controller, this paper considers the combined effects of external interaction force F_{ex} and unknown disturbance d_x acting on the system. The control objective is to stably track the reference velocity trajectory v_d generated by the admittance controller. The following composite controller is constructed:

$$F_m = F_{eq} + F_{sw} - F_{ex} \tag{9}$$

The controller consists of three components:

a) Human–robot interaction feedforward term F_{ex}

The interaction force F_{ex} directly applied by the human is introduced as a feedforward term in the control system, which helps enhance the system's sensitivity and responsiveness in human–robot collaboration [77]–[79]. This whole-body dynamic control structure takes into account the characteristics of human–robot coupling and is more suited to the control needs in active rehabilitation training scenarios.

b) Equivalent control term F_{eq}

This term is used to describe the ideal system dynamics (excluding disturbances and uncertainties), and is designed based on the differentiation of the sliding surface under the condition $\dot{s} = 0$, yielding:

$$F_{eq} = m(\dot{v}_d + \lambda \dot{e} + \rho_e) \tag{10}$$

This term ensures that the system can accurately track the reference trajectory under disturbance-free conditions, serving as the main component of the controller.

c) Sliding mode robust compensation term F_{sw}

This term is used to suppress unknown disturbances d_x, modeling errors, and other uncertainties, and is constructed as follows:

$$F_{sw} = \hat{d}_x + K_s \cdot \frac{s}{\phi + \beta|s|} \tag{11}$$

Where $\hat{d}_x$ is the estimated value of the unknown disturbance d_x by the disturbance observer; K_s is the adaptive sliding mode gain, which dynamically adjusts according to the error dynamics; $\phi > 0$ is the boundary layer parameter, $\beta > 0$ is the frequency tuning parameter.

The sliding mode term adopts a continuous fractional function form:

$$\frac{s}{\phi + \beta|s|}$$

which can effectively alleviate the chattering problem caused by traditional sign functions, while maintaining sufficient robustness.

3) Disturbance Observer Design

To improve accuracy and smoothness, a disturbance observer is introduced to estimate external disturbances in real time, allowing the controller to adjust accordingly [80]–[82]. To reduce the chattering caused by sliding mode switching and improve steady-state performance, a linear disturbance observer is designed to estimate the total disturbance term d_x. Let the estimated disturbance be denoted by $\hat{d}_x$, and based on inverse dynamics, the disturbance observer is constructed as:

$$\hat{d}_x = F_m + F_{ex} - m\dot{v}_i \tag{12}$$

4) Adaptive Sliding Mode Gain Adjustment

To balance system responsiveness and robust control performance, this paper adopts a concise and effective linear adaptive gain design strategy:

$$K_s = K_0 + k_1 \cdot |s| \tag{13}$$

Where $K_0 > 0$ is the base sliding gain, providing minimum control capability; $k_1 > 0$ is the responsiveness factor for sliding mode gain adjustment; $|s|$ Indicates the current deviation magnitude of the sliding surface.

As shown in Fig. 2, the proposed control system for the rehabilitation robot adopts a dual-loop architecture. The outer loop employs an admittance controller to convert the interaction force F_{ex} exerted by the patient into a desired velocity v_d, thereby enabling compliant and natural human–robot interaction. The inner loop consists of an adaptive sliding mode controller (ASMC), which ensures accurate tracking of the desired velocity. A disturbance observer (DO) is integrated to estimate model uncertainties and external disturbances in real time, enhancing the robustness of the control system.

a) The control process is as follows:

The interaction force F_{ex} is applied to the handle of the robot. The admittance controller computes the corresponding desired velocity v_d. The actual velocity v is compared with v_d to obtain the tracking error $e = v_d - v$, which is then fed into the adaptive sliding mode controller. The controller dynamically adjusts the sliding mode gain based on the error evolution. The control law combines the equivalent control term, sliding mode compensation, and disturbance estimation to generate the control signal. The actuator executes the control input, driving the system while being subject to external disturbances.

To mitigate the influence of such disturbances, the disturbance observer estimates the total disturbance in real time based on the system's velocity and applied control force. This estimation is fed back into the control law for compensation. The entire structure forms a closed-loop control system that ensures high-precision and robust velocity tracking performance even in the presence of external disturbances and model uncertainties.

E. Lyapunov Stability Analysis

To mathematically guarantee that the system remains stable despite disturbances, we use Lyapunov theory, a standard method for proving convergence and robustness in control systems [83]–[85]. To verify the stability of the proposed adaptive sliding mode controller under conditions of model uncertainties and external disturbances, the Lyapunov method is employed for analysis. The following Lyapunov function is selected as a candidate function:

$$V = \frac{1}{2}s^2 + \frac{1}{2\gamma}(K_s - Ks^*)^2 + \frac{1}{2}\tilde{d}_x{}^2 \tag{14}$$

where $\tilde{d}_x = d_x - \hat{d}_x$ is the disturbance estimation error, and Ks^* denotes the minimum switching gain required to completely reject the actual disturbance.

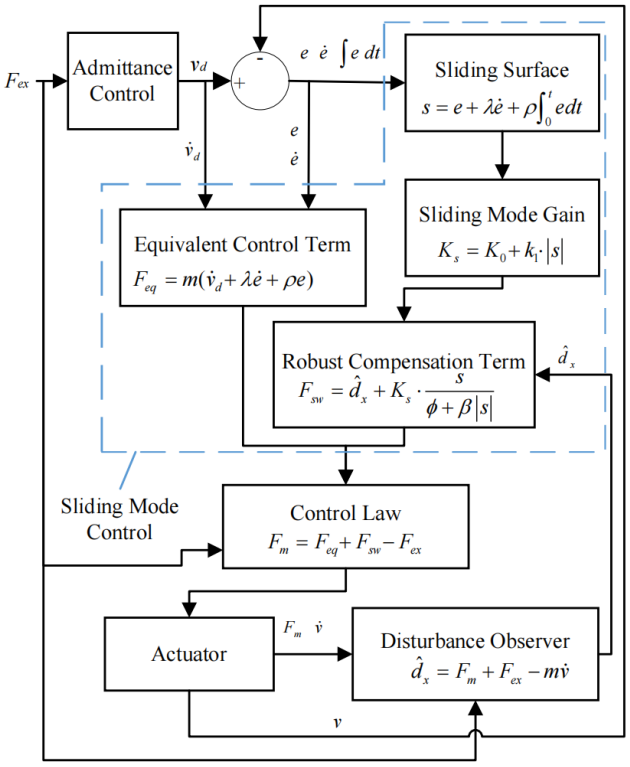

Fig. 2. Dual-loop control architecture with admittance and adaptive SMC

Taking the time derivative of V, we obtain:

$$\dot{V} = s \cdot \dot{s} + \frac{1}{\gamma}(K_s - K_s{}^*)\dot{K}_s + \frac{1}{L_i}\tilde{d}_x\dot{\tilde{d}}_x \tag{15}$$

Each term in the Lyapunov function derivative $\dot{V}$ is analyzed for its sign to ensure that the Lyapunov derivative is negative definite.

a) First term: $s \cdot \dot{s}$

Due to the design of SMC, the tracking error e_i gradually decreases over time, causing s to approach zero.

The design of the sliding mode gain ensures that $\dot{s}$ decreases continuously and eventually tends to zero.

According to SMC theory, the evolution of the sliding surface s and its $\dot{s}$ can be expressed using the following inequalities:

$$|s| \le C_1$$

$$|\dot{s}| \le C_2|s|$$

Therefore, $s \cdot \dot{s}$ can be expressed as:

$$s \cdot \dot{s} \le -\alpha_1 s^2$$

b) Second term: $\frac{1}{\gamma}(K_s - K_s{}^*)\dot{K}_s$

The gain K_s is dynamically adjusted by the control law, so its rate of change $\dot{K}_s$ is related to the error between gains $K_s - K_s{}^*$. The difference $K_s - K_s{}^*$ gradually decreases and can be expressed using the following inequality:

$$|K_s - K_s{}^*| \le C_3$$

$$\left|\dot{K}_s\right| \le C_4|K_s - K^*{}_s|$$

Therefore, the gain term $\frac{1}{\gamma}(K_s - K_s^*)\dot{K}_s$ can be expressed as:

$$\frac{1}{\gamma}(K_s - K_s^*)\dot{K}_s \leq -\alpha_2(K_s - K_s^*)^2$$

c) Third term: $\tilde{d}_x\dot{\tilde{d}}_x$

The disturbance estimation error $\tilde{d}_x$ will gradually approach the actual disturbance based on the system dynamics, and its derivative will also gradually tend to zero. Due to the design of the disturbance estimation, $\tilde{d}_x\dot{\tilde{d}}_x$ will tend to zero. Therefore, it can be concluded that:

$$\tilde{d}_x\dot{\tilde{d}}_x \leq -\alpha_3\tilde{d}_x^2$$

d) Comprehensive Analysis

By combining the three terms, we obtain:

$$\dot{V} \leq -\alpha_1 s^2 - \alpha_2(K_s - K_s^*)^2 - \alpha_3\tilde{d}_x^2$$

Since each term is negative, the derivative of the Lyapunov function is always less than zero. Therefore:

$$\dot{V} \leq -\alpha s^2$$

In summary, the proposed adaptive sliding mode controller ensures closed-loop system stability under the presence of external disturbances and system uncertainties. The tracking error asymptotically converges to zero, and the disturbance estimation error also converges to zero, thereby achieving global asymptotic stability of the system.

Despite incorporating adaptive gain tuning and a disturbance observer, the proposed dual-loop control architecture remains computationally efficient. All control laws are algebraic and rely on first-order derivatives or integrals, making them suitable for real-time implementation. Although the current study focuses on simulation and early-stage experiments, a preliminary deployment analysis suggests that the control algorithm can be implemented on common embedded platforms such as ARM Cortex-M microcontrollers. Future work will include precise timing evaluation and code optimization for hardware deployment.

III. EXPERIMENTS AND DISCUSSION

To verify the effectiveness of the proposed admittance–adaptive SMC strategy, simulation experiments were conducted on the rehabilitation robot system. In order to evaluate the compliance of the admittance control strategy and the robustness of the proposed adaptive sliding mode controller (ASMC) in suppressing unknown frictional disturbances, MATLAB-based simulation experiments were first carried out [86].

A. Admittance and Super Sliding Mode Combined Control

The control parameters are listed in Table 1. To evaluate the performance of the proposed control method under both smooth and abrupt disturbance conditions, a comprehensive simulation scenario was constructed. Specifically, a periodic interaction force F_m＝10cos（2π*0.5t） and a sinusoidal disturbance d_x=3sin（2π*0.5t） were applied to the system. Additionally, a step disturbance of 3 N was introduced at t=4s to simulate sudden external interference. The combined effects of these inputs aim to verify the compliance and robustness of the proposed controller. The corresponding simulation results are shown in Fig. 3.

TABLE I. SIMULATION CONTROL SYSTEM PARAMETERS

Parameter Name	Symbol	Value	Unit
Physical mass	m	2	kg
Proportional gain	λ	12	
Integral gain	ρ	66	
Boundary layer parameter	ϕ	0.2	
Frequency parameter	β	0.5	
Admittance mass	m_d	0.5	kg
Admittance mass	b_d	4	$N \cdot s/m$
Admittance mass	K_0	1	——
Gain ratio	k_1	5	

- Fig. 3(a): Shows the consistency between the handle's motion velocity and the desired velocity, reflecting excellent tracking performance under compliant control. The actual speed closely follows the sinusoidal reference trajectory across the entire duration.
- Fig. 3(b): Illustrates the comparison between the actual disturbance and the estimated disturbance. The green dashed curve almost completely overlaps the true disturbance, confirming that the disturbance observer achieves high accuracy in real-time estimation.
- Fig. 3(c): Displays the time evolution of the sliding surface s. A red rectangle highlights the transient peak caused by the step disturbance at 4s. The inset plot provides a magnified view of this region, showing how s spikes sharply before rapidly converging back toward zero. This behavior demonstrates the strong disturbance rejection capability and fast error attenuation of the proposed adaptive sliding mode controller.
- Fig. 3(d): Depicts the variation of the adaptive sliding gain K_s over time. A blue rectangle marks the disturbance response region, and the zoomed inset shows a sharp gain increase in response to the error spike. Subsequently, K_s decreases smoothly and stabilizes, confirming that the adaptive gain mechanism dynamically adjusts control strength based on the error magnitude. This ensures accurate and robust tracking even under sudden disturbances.

To quantitatively evaluate the superiority of the proposed control strategy compared to conventional PID control, a baseline PID controller was implemented with identical system parameters. The proportional, integral, and derivative gains were set to K_p=40, K_i=5, and K_d=1.5, respectively. Fig. 4 presents a comparison of the velocity tracking errors between the proposed controller and the PID approach under the same external force and disturbance conditions.

Furthermore, three key performance metrics were computed based on simulation data to assess the control effectiveness: (1) the root mean square error (RMSE) of the tracking velocity, (2) the maximum tracking error under disturbance, and (3) the recovery time, defined as the duration required for the tracking error to return within a ±0.05 m/s threshold after the application of a step disturbance. The

quantitative results of both control schemes are summarized in Table II.

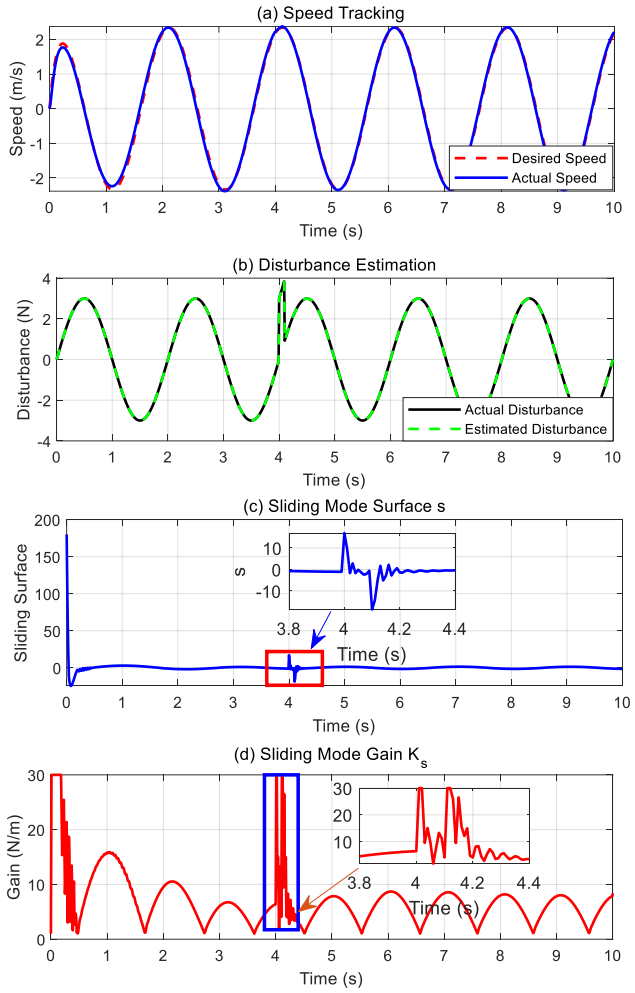

Fig. 3. Simulation results of admittance and adaptive SMC

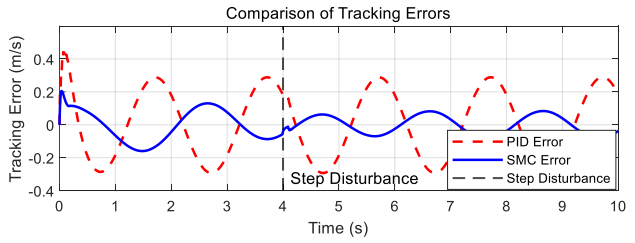

Fig. 4. Tracking error comparison: PID vs. SMC

TABLE II. PERFORMANCE COMPARISON BETWEEN PID AND ADAPTIVE SMC CONTROLLERS

Method	RMSE(m/s)	Max Error(m/s)	Recover Time(s)
PID	0.2113	0.4553	0.81
ASMC+DO	0.0747	0.2057	1.26

Compared to PID control, the proposed controller achieved: A 64.6% reduction in RMSE (from 0.2113 m/s to 0.0747 m/s), A 54.8% reduction in maximum error (from 0.4553 m/s to 0.2057 m/s), and A shorter recovery time (from 1.26 s to 0.81 s) following a step disturbance.

These findings confirm that the proposed controller achieves not only excellent tracking accuracy and improved system stability, but also stronger robustness. The RMSE is significantly lower than that of conventional control methods, reflecting reliable trajectory tracking performance. The disturbance observer enhances compensation accuracy, while the sliding surface rapidly converges during disturbances, ensuring precise dynamic response. In addition, the adaptive adjustment of the sliding gain k_s enables the controller to dynamically regulate control strength—intensifying control when large errors occur and reducing it as the system stabilizes—thus achieving both accuracy and smoothness.

B. Experimental Validation

To further verify the effectiveness of the proposed control method, experimental validation was carried out on an upper-limb rehabilitation robot.

Fig. 5 shows the compliant control of the handle during active training mode. A force sensor installed at the bottom of the handle was used to detect the participant's training intention. The motor drives the handle to follow the interaction force in a compliant manner.

Fig. 5. Prototype experimental verification

In Fig. 5, a rubber band is fixed to the handle, and only a small interaction force is needed to realize compliant motion following.

As shown clearly in Fig. 6, the handle velocity dynamically follows the changes in interaction force, demonstrating the compliant force–velocity mapping of the robot.

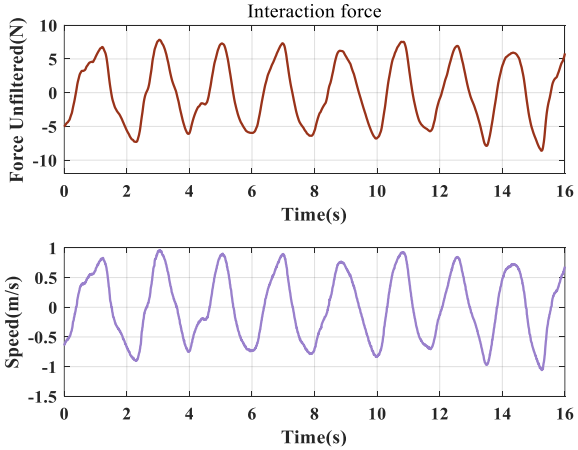

Fig. 6. Variation curves of robot interaction force and velocity

The experimental results confirm that the handle can respond rapidly to changes in interaction force while maintaining stable motion, thereby validating the effectiveness of the combined admittance and adaptive SMC strategy. The experiment was conducted using a healthy adult male (age: 28) in active tracking mode. A rubber band was used to simulate compliant resistance. The system's sampling frequency was 1 kHz, and the force sensor had an accuracy of ±0.1 N.

VI. CONCLUSION

This paper proposes a robust velocity control method with adaptive disturbance compensation for rehabilitation robots, aiming to achieve compliant velocity tracking during patient-initiated movement. The control strategy adopts a dual-loop architecture: an outer-loop admittance controller enables the robot to respond compliantly to external forces applied by the patient, imparting a desired mass–damping behavior to the system; an inner-loop adaptive sliding mode controller ensures high-precision and robust velocity tracking under model uncertainties and external disturbances. The combination of adaptive sliding mode control and a disturbance observer significantly mitigates the chattering problem commonly associated with traditional sliding mode control.

The proposed control strategy offers a key advantage by integrating compliant human–robot interaction with robust and precise control performance:

- The outer-loop admittance controller allows the robot handle to actively follow the patient's motion intention;
- The inner-loop adaptive sliding mode controller ensures accurate velocity tracking even under varying patient forces and disturbances.

This dual-loop structure is particularly suitable for rehabilitation training scenarios, as it enhances the intensity of active movement while maintaining the accuracy and safety of execution. Simulation and preliminary experimental results validate the effectiveness of the proposed method in improving response speed, tracking precision, and disturbance rejection capability.

Nonetheless, several limitations remain in the current study:

- The system is limited to a planar two-degree-of-freedom (2-DOF) configuration, consisting of two perpendicular translational axes, which restricts its functionality;
- The modeling of human input signals, such as motion intention, is simplified and may not fully reflect the complexity of real-world human–robot interaction;
- Clinical validation has not yet been conducted, and the method lacks experimental data from actual patients.

Future research will focus on:

- Extending the control framework to multi-degree-of-freedom (multi-DOF) systems, enabling 3D rehabilitation motion control;
- Integrating patient-specific physiological signals, such as electromyography (EMG) or intention recognition, to make the control strategy more intelligent and personalized.

In conclusion, the proposed adaptive disturbance-compensated robust velocity control method provides an effective solution for active rehabilitation training. It achieves a balance between compliant human–robot interaction and robust control performance, and holds strong potential for application in other types of rehabilitation robots, contributing to improved patient engagement and rehabilitation outcomes.

REFERENCES

[1] W. Ding, S. Hu, P. Wang, H. Kang, R. Peng, Y. Dong, and F. Li, "Spinal cord injury: the global incidence, prevalence, and disability from the global burden of disease study 2019," *Spine*, vol. 47, no. 21, pp. 1532–1540, 2022.

[2] M. Zhang, X. Han, L. Yan, Y. Fu, H. Kou, C. Shang, and T. Cheng, "Inflammatory response in traumatic brain and spinal cord injury: The role of XCL1–XCR1 axis and T cells," *CNS Neurosci Ther*, vol. 30, no. 6, p. e14781, 2024.

[3] V. L. Feigin, T. Vos, E. Nichols, M. O. Owolabi, W. M. Carroll, M. Dichgans, and C. Murray, "The global burden of neurological disorders: translating evidence into policy," *Lancet Neurol*, vol. 19, no. 3, pp. 255–265, 2020.

[4] N. Hugues, C. Pellegrino, C. Rivera, E. Berton, C. Pin-Barre, and J. Laurin, "Is high-intensity interval training suitable to promote neuroplasticity and cognitive functions after stroke," *Int J Mol Sci*, vol. 22, no. 6, p. 3003, 2021.

[5] R. G. Braun and G. F. Wittenberg, "Motor recovery: How rehabilitation techniques and technologies can enhance recovery and neuroplasticity," *Semin Neurol*, vol. 41, no. 2, pp. 167–176, Apr. 2021.

[6] S. F. Atashzar, J. Carriere, and M. Tavakoli, "How can intelligent robots and smart mechatronic modules facilitate remote assessment, assistance, and rehabilitation for isolated adults with neuro-musculoskeletal conditions?," *Front. Robot. AI*, vol. 8, p. 610529, 2021.

[7] R. Zhang, Y. Zhou, J. Zhang, and J. Zhao, "Cloud-integrated robotics: transforming healthcare and rehabilitation for individuals with disabilities," *Proc. Indian Natl. Sci. Acad.*, vol. 90, no. 3, pp. 752–763, Sep. 2024.

[8] E. Godecke, E. Armstrong, T. Rai, N. Ciccone, M. L. Rose, S. Middleton, and V. C. Group, "A randomized control trial of intensive aphasia therapy after acute stroke: The Very Early Rehabilitation for SpEech (VERSE) study," *Int J Stroke*, vol. 16, no. 5, pp. 556–572, 2021.

[9] A. Garcia-Gonzalez, R. Q. Fuentes-Aguilar, I. Salgado, and I. Chairez, "A review on the application of autonomous and intelligent robotic devices in medical rehabilitation," *J Braz Soc Mech Sci Eng*, vol. 44, no. 9, p. 393, 2022.

[10] D. Mukherjee, K. Gupta, L. H. Chang, and H. Najjaran, "A survey of robot learning strategies for human-robot collaboration in industrial settings," *Robot Comput-Integr Manuf*, vol. 73, p. 102231, 2022.

[11] J. B. Lara, M. Tsoukas, and K. Avanaki, "Tumor assessment system using high frequency ultrasound and photoacoustic imaging: system development," in *Photons Plus Ultrasound: Imaging and Sensing 2024*, vol. 12842, pp. 275–281, 2024.

[12] C. Wang, E. Shirzaei Sani, C.-D. Shih, C. T. Lim, J. Wang, D. G. Armstrong, and W. Gao, "Wound management materials and technologies from bench to bedside and beyond," *Nat. Rev. Mater.*, vol. 9, no. 8, pp. 550–566, 2024.

[13] P. F. Wilson, M. Gilany, A. Jamzad, F. Fooladgar, M. N. N. To, B. Wodlinger, P. Abolmaesumi, and P. Mousavi, "Self-supervised learning with limited labeled data for prostate cancer detection in high-frequency ultrasound," *IEEE Trans. Ultrason. Ferroelectr. Freq. Control*, vol. 70, no. 9, pp. 1073–1083, 2023.

[14] V. Palaniappan, I. Ishak, H. Ibrahim, F. Sidi, and Z. A. Zukarnain, "A Review on High-Frequency Trading Forecasting Methods:

Opportunity and Challenges for Quantum Based Method," in *IEEE Access*, vol. 12, pp. 167471-167488, 2024.

[15] M. Sharifi, V. Azimi, V. K. Mushahwar, and M. Tavakoli, "Impedance learning-based adaptive control for human–robot interaction," *IEEE Trans. Control Syst. Technol.*, vol. 30, no. 4, pp. 1345–1358, 2021.

[16] F. Gongor and O. Tutsoy, "On the Remarkable Advancement of Assistive Robotics in Human-Robot Interaction-Based Health-Care Applications: An Exploratory Overview of the Literature," *Int. J. Human–Computer Interact.*, vol. 41, no. 2, pp. 1502–1542, Jan. 2025.

[17] A. Gvion and G. Shahaf, "Real-time monitoring of barriers to patient engagement for improved rehabilitation: a protocol and representative case reports," *Disabil Rehabil Assist Technol*, vol. 18, no. 6, pp. 849–861, 2023.

[18] R. Yang, J. Zheng, and R. Song, "Continuous mode adaptation for cable-driven rehabilitation robot using reinforcement learning," *Front. Neurorobotics*, vol. 16, p. 1068706, 2022.

[19] Q. Wu and Y. Chen, "Variable admittance time-delay control of an upper limb rehabilitation robot based on human stiffness estimation," *Mechatronics*, vol. 90, p. 102935, 2023.

[20] H. Shen, X. Liu, K. Liu, Y. Yao, X. Weng, and L. Yang, "Research on compliant human–robot interaction based on admittance control strategy for shoulder rehabilitation exoskeleton with CGH self-alignment function," *Int. J. Intell. Robot. Appl.*, vol. 8, no. 3, pp. 692–708, Sep. 2024.

[21] M. F. Shah, S. Hussain, R. Goecke, and P. K. Jamwal, "Mechanism design and control of shoulder rehabilitation robots: A review," *IEEE Trans. Med. Robot. Bionics*, vol. 5, no. 4, pp. 780–792, 2023.

[22] K. Maqsood, J. Luo, C. Yang, Q. Ren, and Y. Li, "Iterative learning-based path control for robot-assisted upper-limb rehabilitation," *Neural Comput. Appl.*, vol. 35, no. 32, pp. 23329–23341, Nov. 2023.

[23] Q. Wu, B. Chen, and H. Wu, "Adaptive admittance control of an upper extremity rehabilitation robot with neural-network-based disturbance observer," *IEEE Access*, vol. 7, pp. 123807–123819, 2019.

[24] M. Briguglio, "Nutritional orthopedics and space nutrition as two sides of the same coin: A scoping review," *Nutrients*, vol. 13, no. 2, p. 483, 2021.

[25] Y. Zhuang, S. Yao, C. Ma, and R. Song, "Admittance control based on EMG-driven musculoskeletal model improves the human–robot synchronization," *IEEE Trans Ind Inf.*, vol. 15, no. 2, pp. 1211–1218, 2018.

[26] T. Wang, H. Parwana, K. Umemoto, T. Endo, and F. Matsuno, "Non-cascade Adaptive Sliding Mode Control for Quadrotor UAVs under Parametric Uncertainties and External Disturbance with Indoor Experiments," *J. Intell. Robot. Syst.*, vol. 102, no. 1, p. 8, May 2021.

[27] F. Wang, J. Wang, K. Wang, Q. Zong, and C. Hua, "Adaptive Backstepping Sliding Mode Control of Uncertain Semi-Strict Nonlinear Systems and Application to Permanent Magnet Synchronous Motor," *J. Syst. Sci. Complex.*, vol. 34, no. 2, pp. 552–571, Apr. 2021.

[28] A. Ullah, S. Ullah, T. U. Rahman, I. Sami, A. U. Rahman, B. Alghamdi, and J. Pan, "Enhanced wind energy conversion system performance using fast smooth second-order sliding mode control with neuro-fuzzy estimation and variable-gain robust exact output differentiator," *Appl. Energy*, vol. 377, p. 124364, 2025.

[29] M. Salman, Z. Niu, R. Singh, L. Kshetrimayum, and I. Hussain, "Robust control of a compliant manipulator with reduced dynamics and sliding perturbation observer," *Sci. Rep.*, vol. 15, no. 1, p. 8934, 2025.

[30] O. Mechali, L. Xu, Y. Huang, M. Shi, and X. Xie, "Observer-based fixed-time continuous nonsingular terminal sliding mode control of quadrotor aircraft under uncertainties and disturbances for robust trajectory tracking: Theory and experiment," *Control Eng. Pract.*, vol. 111, p. 104806, 2021.

[31] B. Brahmi, I. E. Bojairami, M. Saad, M. Driscoll, S. Zemam, and M. H. Laraki, "Enhancement of sliding mode control performance for perturbed and unperturbed nonlinear systems: Theory and experimentation on rehabilitation robot," *J Electr Eng Technol*, vol. 16, pp. 599–616, 2021.

[32] G. Zhu, S. Wang, L. Sun, W. Ge, and X. Zhang, "Output feedback adaptive dynamic surface sliding-mode control for quadrotor UAVs with tracking error constraints," *Complexity*, vol. 2020, no. 1, p. 8537198, 2020.

[33] M. S. Khan and R. K. Mandava, "A review on gait generation of the biped robot on various terrains," *Robotica*, vol. 41, no. 6, pp. 1888–1930, 2023.

[34] T. Li, H. Xing, E. Hashemi, H. D. Taghirad, and M. Tavakoli, "A brief survey of observers for disturbance estimation and compensation," *Robotica*, vol. 41, no. 12, pp. 3818–3845, 2023.

[35] M. Asperti, M. Vignati, and E. Sabbioni, "On torque vectoring control: review and comparison of state-of-the-art approaches," *Machines*, vol. 12, no. 3, p. 160, 2024.

[36] A. Kasiri and F. Fani Saberi, "Coupled position and attitude control of a servicer spacecraft in rendezvous with an orbiting target," *Sci. Rep.*, vol. 13, no. 1, p. 4182, 2023.

[37] W. Cai, Z. Liu, M. Zhang, and C. Wang, "Cooperative Artificial Intelligence for underwater robotic swarm," *Robot. Auton. Syst.*, vol. 164, p. 104410, 2023.

[38] M. Hermassi, S. Krim, Y. Kraiem, and M. A. Hajjaji, "Adaptive neuro fuzzy technology to enhance PID performances within VCA for grid-connected wind system under nonlinear behaviors: FPGA hardware implementation," *Comput. Electr. Eng.*, vol. 117, p. 109264, 2024.

[39] V. Moskalenko, V. Kharchenko, A. Moskalenko, and B. Kuzikov, "Resilience and resilient systems of artificial intelligence: taxonomy, models and methods," *Algorithms*, vol. 16, no. 3, p. 165, 2023.

[40] C. Song, G. Liu, C. Li, and J. Zhao, "Reactive task adaptation of a dynamic system with external disturbances based on invariance control and movement primitives," *IEEE Trans. Cogn. Dev. Syst.*, vol. 14, no. 3, pp. 1082–1091, 2021.

[41] Q. Zhu and T. Başar, "Disentangling resilience from robustness: Contextual dualism, interactionism, and game-theoretic paradigms," *IEEE Control Syst. Mag.*, vol. 44, no. 3, pp. 95–103, 2024.

[42] X.-B. Jin, R. J. Robert Jeremiah, T.-L. Su, Y.-T. Bai, and J.-L. Kong, "The new trend of state estimation: From model-driven to hybrid-driven methods," *Sensors*, vol. 21, no. 6, p. 2085, 2021.

[43] D. Guha, P. K. Roy, and S. Banerjee, "Adaptive fractional-order sliding-mode disturbance observer-based robust theoretical frequency controller applied to hybrid wind–diesel power system," *ISA Trans.*, vol. 133, pp. 160–183, 2023.

[44] R. Gehlhar, M. Tucker, A. J. Young, and A. D. Ames, "A review of current state-of-the-art control methods for lower-limb powered prostheses," *Annu. Rev. Control*, vol. 55, pp. 142–164, 2023.

[45] P. Sebastjan and W. Kuś, "Method for parameter tuning of hybrid optimization algorithms for problems with high computational costs of objective function evaluations," *Appl. Sci.*, vol. 13, no. 10, p. 6307, 2023.

[46] H. Sorouri, A. Oshnoei, Y. Che, and R. Teodorescu, "A comprehensive review of hybrid battery state of charge estimation: Exploring physics-aware AI-based approaches," *J. Energy Storage*, vol. 100, p. 113604, 2024.

[47] J. Cao, J. Zhang, C. Wang, K. Li, J. Zhang, G. Wang, and H. Ren, "Variable Admittance Control of High Compatibility Exoskeleton Based on Human–Robotic Interaction Force," *Chin. J. Mech. Eng.*, vol. 37, no. 1, p. 119, Oct. 2024.

[48] X. Shu, F. Ni, K. Min, Y. Liu, and H. Liu, "A novel dual-arm adaptive cooperative control framework for carrying variable loads and active anti-overturning," *ISA Trans.*, vol. 148, pp. 477–489, 2024.

[49] Y. Zhou, C.-Y. Chen, G. Yang, and C. Zhang, "Finite-time SMC-based admittance controller design of macro-micro robotic system for complex surface polishing operations," *Robot. Comput.-Integr. Manuf.*, vol. 92, p. 102881, 2025.

[50] A. Kalibala, A. A. Nada, H. Ishii, and H. El-Hussieny, "Real-time force/position control of soft growing robots: A data-driven model predictive approach," *Nonlinear Eng.*, vol. 14, no. 1, p. 20250099, Mar. 2025.

[51] Y. Du, S. Zhang, Z. Zhang, and H. Wang, "Shape deformation analysis and dynamic modeling of a switchable rigid-continuum robot," *Robotica*, pp. 1–23, 2024.

[52] D. Rakestraw, D. Higgins, D. Harris, M. Allen, E. Red, D. Lang, M. Gamez, and D. A. Strubbe, "Exploring Newton's second law and kinetic friction using the accelerometer sensor in smartphones," *Phys. Teach.*, vol. 61, no. 6, pp. 473–476, 2023.

[53] Y. Jiang, B. Han, X. Liu, M. Han, J. Yao, and Y. Zhao, "Finite-step-integration: An original method for the forward kinematics analysis of

parallel manipulators," *Front. Mech. Eng.*, vol. 20, no. 1, p. 7, Feb. 2025.

[54] J. Leng, J. Guo, J. Xie, X. Zhou, A. Liu, X. Gu, D. Mourtzis, Q. Qi, Q. Liu, and W. Shen, "Review of manufacturing system design in the interplay of Industry 4.0 and Industry 5.0 (Part I): Design thinking and modeling methods," *J. Manuf. Syst.*, vol. 76, pp. 158–187, 2024.

[55] C. Li, M. Xu, W. Song, and H. Zhang, "A review of static and dynamic analysis of ball screw feed drives, recirculating linear guideway, and ball screw," *Int. J. Mach. Tools Manuf.*, vol. 188, p. 104021, 2023.

[56] Y. Luo, J. Gao, F. Feng, Y. Liu, D. Chen, L. Zhang, and X. Chen, "An Innovative Pose Decoupling Calibration Method for Five-Axis Hybrid Mechanism Through Rotation Vector Equivalence," *IEEE Trans. Ind. Electron.*, 2025.

[57] H. Zhong, X. Li, L. Gao, and C. Li, "Toward safe human–robot interaction: A fast-response admittance control method for series elastic actuator," *IEEE Trans. Autom. Sci. Eng.*, vol. 19, no. 2, pp. 919–932, 2021.

[58] D. Ye, C. Yang, Y. Jiang, and H. Zhang, "Hybrid impedance and admittance control for optimal robot–environment interaction," *Robotica*, vol. 42, no. 2, pp. 510–535, 2024.

[59] H. Xing, A. Torabi, L. Ding, H. Gao, Z. Deng, V. K. Mushahwar, and M. Tavakoli, "An admittance-controlled wheeled mobile manipulator for mobility assistance: Human–robot interaction estimation and redundancy resolution for enhanced force exertion ability," *Mechatronics*, vol. 74, p. 102497, 2021.

[60] T. Fujiki and K. Tahara, "Series admittance–impedance controller for more robust and stable extension of force control," *ROBOMECH J.*, vol. 9, no. 1, p. 23, Dec. 2022.

[61] C. Xie, Q. Yang, Y. Huang, S. W. Su, T. Xu, and R. Song, "A hybrid arm-hand rehabilitation robot with EMG-based admittance controller," *IEEE Trans. Biomed. Circuits Syst.*, vol. 15, no. 6, pp. 1332–1342, 2021.

[62] A. Topini, W. Sansom, N. Secciani, L. Bartalucci, A. Ridolfi, and B. Allotta, "Variable admittance control of a hand exoskeleton for virtual reality-based rehabilitation tasks," *Front. Neurorobotics*, vol. 15, p. 789743, 2022.

[63] X. Xiong, Y. Bai, R. Shi, S. Kamal, Y. Wang, and Y. Lou, "Discrete-time twisting algorithm implementation with implicit-Euler ZOH discretization method," *IEEE Trans. Circuits Syst. II Express Briefs*, vol. 69, no. 8, pp. 3435–3439, 2022.

[64] Y. Ji and Y. Xing, "Highly accurate and efficient time integration methods with unconditional stability and flexible numerical dissipation," *Mathematics*, vol. 11, no. 3, p. 593, 2023.

[65] D. Wang, J. Wang, A. Liu, D. Liu, and J. Qiao, "Relaxed Optimal Control With Self-Learning Horizon for Discrete-Time Stochastic Dynamics," *IEEE Trans. Cybern.*, 2025.

[66] P. M. Wensing, M. Posa, Y. Hu, A. Escande, N. Mansard, and A. Del Prete, "Optimization-based control for dynamic legged robots," *IEEE Trans. Robot.*, vol. 40, pp. 43–63, 2023.

[67] J. A. Rojas-Quintero, J. Villalobos-Chin, and V. Santibanez, "Optimal control of robotic systems using finite elements for time integration of covariant control equations," *IEEE Access*, vol. 9, pp. 104980–105001, 2021.

[68] M. Morlock, N. Meyer, M.-A. Pick, and R. Seifried, "Real-time trajectory tracking control of a parallel robot with flexible links," *Mech. Mach. Theory*, vol. 158, p. 104220, 2021.

[69] Y. Xiang, P. Tan, H. He, J. Shang, and Y. Zhang, "Seismic optimization of variable friction pendulum tuned mass damper with hysteretic damping characteristic," *Soil Dyn. Earthq. Eng.*, vol. 160, p. 107381, 2022.

[70] A. Wilk, L. Gelman, S. Judek, K. Karwowski, M. Mizan, T. Maciołek, M. Lewandowski, A. Jakubowski, and K. Klimowska, "Novel method of estimation of inertial and dissipative parameters of a railway pantograph model," *Veh. Syst. Dyn.*, vol. 60, no. 7, pp. 2413–2435, Jul. 2022.

[71] R.-D. Xi, X. Xiao, T.-N. Ma, and Z.-X. Yang, "Adaptive sliding mode disturbance observer based robust control for robot manipulators towards assembly assistance," *IEEE Robot. Autom. Lett.*, vol. 7, no. 3, pp. 6139–6146, 2022.

[72] D. Tian, R. Xu, E. Sariyildiz, and H. Gao, "An adaptive switching-gain sliding-mode-assisted disturbance observer for high-precision servo control," *IEEE Trans. Ind. Electron.*, vol. 69, no. 2, pp. 1762–1772, 2021.

[73] N. Ahmed and M. Chen, "Disturbance observer-based robust adaptive control for uncertain actuated nonlinear systemwith disturbances," *Assem. Autom.*, vol. 41, no. 5, pp. 567–576, 2021.

[74] H. Feng, J. Jiang, X. Chang, C. Yin, D. Cao, H. Yu, C. Li, and J. Xie, "Adaptive sliding mode controller based on fuzzy rules for a typical excavator electro-hydraulic position control system," *Eng. Appl. Artif. Intell.*, vol. 126, p. 107008, 2023.

[75] H. Zhong, X. Li, L. Gao, and C. Li, "Toward safe human–robot interaction: A fast-response admittance control method for series elastic actuator," *IEEE Trans. Autom. Sci. Eng.*, vol. 19, no. 2, pp. 919–932, 2021.

[76] C. Liu, Y. He, X. Chen, and H. Cao, "Adaptive enhanced admittance force-tracking controller design for highly dynamic interactive tasks," *Ind. Robot Int. J. Robot. Res. Appl.*, vol. 49, no. 5, pp. 903–912, 2022.

[77] S. Proia, R. Carli, G. Cavone, and M. Dotoli, "Control techniques for safe, ergonomic, and efficient human-robot collaboration in the digital industry: A survey," *IEEE Trans. Autom. Sci. Eng.*, vol. 19, no. 3, pp. 1798–1819, 2021.

[78] D. Mukherjee, K. Gupta, L. H. Chang, and H. Najjaran, "A survey of robot learning strategies for human-robot collaboration in industrial settings," *Robot. Comput.-Integr. Manuf.*, vol. 73, p. 102231, 2022.

[79] H. Kim and W. Yang, "Variable admittance control based on human–robot collaboration observer using frequency analysis for sensitive and safe interaction," *Sensors*, vol. 21, no. 5, p. 1899, 2021.

[80] Z. Sun, M. Xiao, D. Li, and J. Chu, "Tracking controller design for quadrotor UAVs under external disturbances using a high-order sliding mode-assisted disturbance observer," *Meas. Control*, vol. 58, no. 2, pp. 155–167, Feb. 2025.

[81] H.-S. Lee, J. Back, and C.-S. Kim, "Disturbance observer-based robust controller for a multiple-electromagnets actuator," *IEEE Trans. Ind. Electron.*, vol. 71, no. 1, pp. 901–911, 2023.

[82] S. I. Azid, K. Kumar, M. Cirrincione, and A. Fagiolini, "Robust motion control of nonlinear quadrotor model with wind disturbance observer," *IEEE Access*, vol. 9, pp. 149164–149175, 2021.

[83] Y. Zheng, Q. Li, and S. Li, "Stability guaranteed model predictive control with adaptive Lyapunov constraint," *IEEE Trans. Autom. Sci. Eng.*, vol. 21, no. 1, pp. 215–225, 2022.

[84] H. Zhang, C. Zhao, and J. Ding, "Robust safe reinforcement learning control of unknown continuous-time nonlinear systems with state constraints and disturbances," *J. Process Control*, vol. 128, p. 103028, 2023.

[85] A. Ullah, S. Ullah, T. U. Rahman, I. Sami, A. U. Rahman, B. Alghamdi, and J. Pan, "Enhanced wind energy conversion system performance using fast smooth second-order sliding mode control with neuro-fuzzy estimation and variable-gain robust exact output differentiator," *Appl. Energy*, vol. 377, p. 124364, 2025.

[86] J. Chen, X. Luo, C. Hua, D. Mu, and F. Sun, "Modeling and Robust Adaptive Practical Predefined Time and Precision Tracking Control of Unmanned Fire Fighting Robot," *IEEE Trans. Syst. Man Cybern. Syst.*, 2024.